J. Fluid Mech. (1993), *vol.* 256, *pp.* 315–341

Acoustic forcing of oblique wave resonance in the far wake

By C. H. K. WILLIAMSON AND A. PRASAD
Mechanical and Aerospace Engineering, Upson Hall, Cornell University, Ithaca, NY 14853, USA

(Received 21 December 1992 and in revised form 12 May 1993)

In this paper, we investigate to what extent the far-wake 'signature' of the near-wake vortex dynamics of a nominally two-dimensional bluff body is affected by the character of the free-stream noise. We confirm the existence of an oblique wave resonance (at frequency, $f_K - f_T$), which is caused by nonlinear 'quadratic' interactions between primary oblique shedding waves (f_K) and secondary two-dimensional waves (f_T), which are amplified from free-stream disturbances. In this work, oblique wave resonance is induced by acoustic forcing of two-dimensional waves. The use of acoustic forcing reveals a set of higher-order oblique wave resonances corresponding to frequencies ($f_K - nf_T$), where n is an integer. We find from visualization that, even when the secondary two-dimensional waves have the same frequency as the oblique waves, it is the oblique waves that are preferentially amplified. Oblique wave angles up to 74° have been observed. The response of the wake to a large range of forcing frequencies shows a broad region of peak response, centred around $F = (f_T/f_K) = 0.55$, and is in reasonable agreement with predictions from linear stability analysis. A similar broad response is found for each of the higher-order oblique wave modes. Simple equations for the oblique waves yield approximate conditions for maximum wake response, with a frequency for peak response given by $F_{max} = 1/2n = 1/2,\ 1/4,\ 1/6, \ldots$, and an oblique wave angle given by $\theta_{max} = 2\theta_K$, where θ_K is the angle of oblique vortex shedding. An increase in forcing amplitude has the effect of bringing the nonlinear wave interactions, leading to oblique wave resonance, further upstream. Paradoxically, the effect of an increase in amplitude (A) of the two-dimensional wave forcing is to further amplify the oblique waves in preference to the two-dimensional waves and, under some conditions, to inhibit the appearance of prominent two-dimensional waves where they would otherwise appear. With a variation in forcing amplitude, the amplitude of oblique wave response is found to be closely proportional to $A^{\frac{1}{2}}$. In summary, this investigation confirms the surprising result that it is only through the existence of noise in the free stream that the far wake is 'connected' to the near wake.

1. Introduction

One of the basic questions concerning the far wake of a nominally two-dimensional body, and one that has been raised often recently, is to what extent the far-wake vortical structure is 'connected' to the near-wake vortex structure, or to what extent the far wake is a 'signature' of the body that creates it. In a previous paper (Williamson & Prasad 1993*a*, hereinafter denoted WP), it was found that one such signature in the far wake takes the form of an 'oblique wave resonance', which is triggered by the extreme sensitivity of the flow to free-stream disturbances – *it is surprisingly the noise that actually forges the 'connection' between near and far wakes*, leaving a signature of the body's wake far downstream. Our intent with the present paper is therefore to

investigate how the character of the free stream influences far-wake nonlinear resonances, and in this particular work we shall be concerned with the far-wake response to single-frequency acoustic forcing of the free stream. Three-dimensional resonances will be induced (paradoxically) through the use of two-dimensional forcing. In the far wake, a quadratic nonlinear interaction between the forced two-dimensional secondary waves and 'shed' oblique waves (from the body upstream) is found to trigger the resonance of a third 'oblique resonance wave', confirming the resonance found in WP when a minute peak in the free-stream spectrum was sufficient as the trigger. In the present paper, we shall deliberately vary forcing frequencies and amplitude to study wake response, and we shall show that there exists a set of oblique resonance modes. For each of these modes, we shall find conditions for maximum response, and study the general character of these resonances. The present investigation is conducted with a view to understanding mechanisms of significance to laminar–turbulent transition as well as to far-wake 'signatures'.

In both the laminar and turbulent regimes, the width of a nominally two-dimensional far wake grows as $x^{\frac{1}{2}}$, for large values of downstream distance (x), and we thus expect the size of the large wake structures to increase, while the passage frequency of these structures should decrease. Some original experiments by Taneda (1959) and by Matsui & Okude (1981, 1983) have shown the decay of the original Kármán street wake and the growth in the far wake of a larger-scale secondary vortex street. Although there has been some discussion, based on these studies, as to whether the secondary street growth is due to vortex pairing or to hydrodynamic instability, it appears from the studies of Cimbala (1984), Cimbala, Nagib & Roshko (1988), and Williamson & Prasad (1993*a*) that growth is due to hydrodynamic instability.

Cimbala *et al.* (1988) further discovered a regular three-dimensional 'honeycomb-like' pattern in the far wake. This observation has been the subject of some debate since that time, which is discussed fully in WP. Although there has been a suggestion that the 'honeycomb-like' patterns are due to a parametric subharmonic resonance of the kind found in shear layers and boundary layers (Lasheras & Meiburg 1990; Corke, Krull & Ghassemi 1992), Williamson & Prasad (1993*a*, *b*) have shown that the patterns observed 'naturally' in wind tunnels are due to an interaction between oblique-shedding primary waves (shed from the body upstream) and two-dimensional secondary waves of larger streamwise wavelength (which are unstable and grow downstream). This scenario, shown schematically in figure 1(*b*), is obviously distinct from the subharmonic interactions in figure 1(*a*). In the subharmonic interactions, the primary waves are two-dimensional, while the secondary waves comprise pairs of oblique waves of opposite angle, as distinct from the single sets of primary oblique waves and secondary two-dimensional waves in (*b*). The above discussion does not imply that one cannot induce a subharmonic resonance with suitable three-wave forcing, which has indeed been successfully achieved by previous studies; it does suggest however that far-wake patterns observed to date without deliberate forcing are of the oblique wave resonance type, as shown in figure 1(*b*).

Intrinsic to the oblique resonance, as shown in WP, is the fact that the near and far wakes are connected in both scale and frequency. The characteristic that forges this 'connection' between the near and far wakes is the sensitivity to free-stream disturbances (as mentioned earlier). In the presence of a very small spectral peak (f_T) in the free stream, it is found that the far wake is receptive to a combination-frequency response given by $f_{FW} = (f_K - f_T)$, where f_K is the vortex-shedding frequency. This combination-frequency response corresponds physically with the 'oblique wave resonance', described in WP, and shown schematically in figure 2. The discovery of

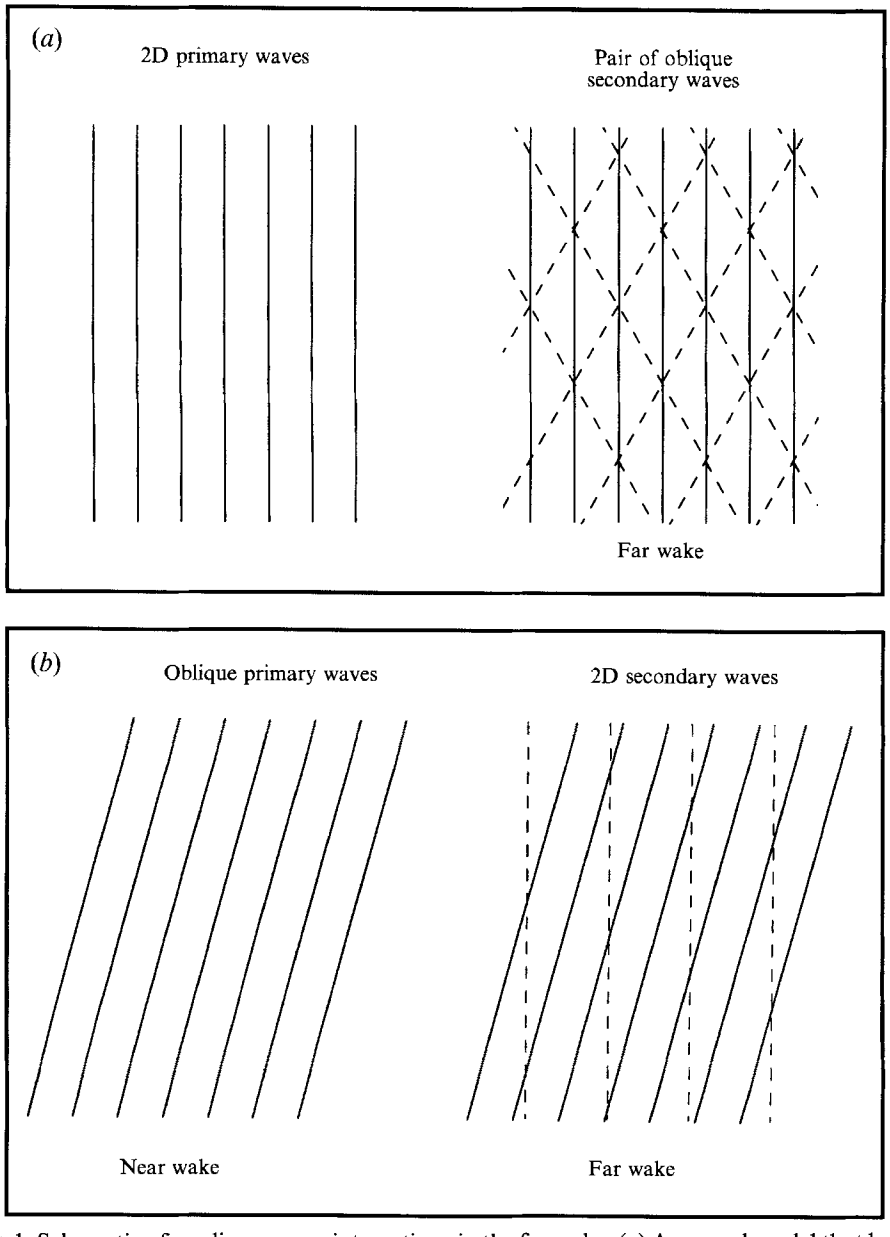

FIGURE 1. Schematic of nonlinear wave interactions in the far wake. (*a*) A general model that has been used to represent far-wake wave interactions involving a subharmonic instability. (*b*) The observed nonlinear wave interactions for the 'naturally' evolving wake.

such a resonance in the far wake has been made possible by a new understanding of near wake three-dimensional phenomena, in particular the observation that oblique vortex shedding itself (where vortices are shed at some angle to the cylinder axis) is caused by influences from the end boundary conditions, for cylinders of even hundreds of diameters in length (Williamson 1988, 1989; Eisenlohr & Eckelmann 1989; Konig, Eisenlohr & Eckelmann 1990; Hammache & Gharib 1989, 1991).

The oblique wave resonance studied in WP was caused by a remarkably small peak in the free-stream spectrum (with a turbulence intensity level of $(u'_{rms}/U) = 0.00005$).

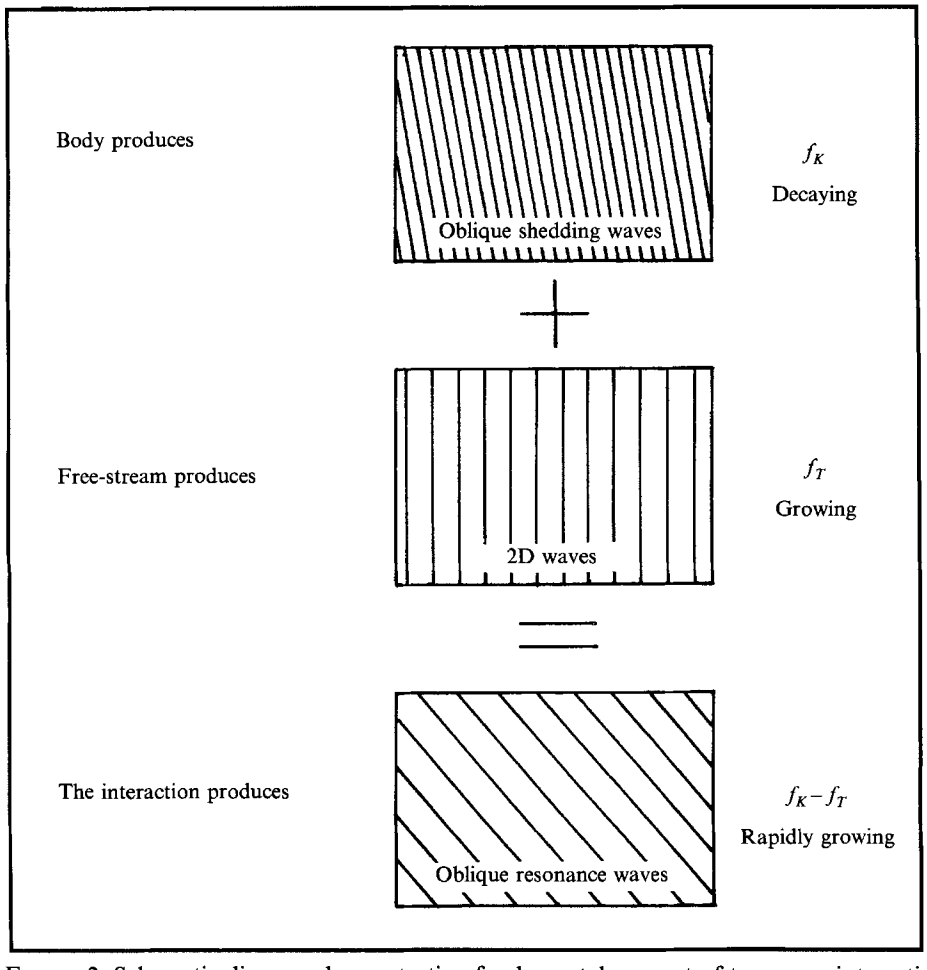

FIGURE 2. Schematic diagram demonstrating fundamental concept of two-wave interaction (f_K and f_T) yielding an oblique resonance wave ($f_K - f_T$).

The discovery that this noise is caused by an acoustic disturbance has stimulated the present acoustic forcing experiments. Our intention is to investigate how the character of the free-stream spectrum influences far-wake resonances. Paradoxically, the secondary oblique waves will be triggered by two-dimensional forcing. With this study, we intend to confirm that oblique waves are prefentially amplified over two-dimensional waves. Indeed, we shall find that increasing the level of the two-dimensional forcing increases the strength of the oblique resonance waves, in preference to the two-dimensional secondary waves! Particular attention will be paid to a frequency ratio of $(f_T/f_K) = 0.5$. At this value, the oblique waves ($f_{\theta 1}$) have precisely the same frequency as the two-dimensional waves (f_T). A major impetus for this study, aside from characterizing the wake response under controlled conditions, is to discover further nonlinear oblique wave resonances in the far wake, which correspond with further combination frequencies.

A related study has been conducted by Desruelle (1983), who acoustically forced the far wake using a speaker, and indeed he found that often the principal response occurred at a combination frequency, rather than at the imposed frequency itself. A similar response comprising a set of combination frequencies was found by Cimbala &

Krein (1990), when they indirectly interfered with the spectral peaks in the free-stream spectrum, by manipulating vents in the test section of their wind tunnel. These studies did not however involve simultaneous spanwise visualization, but it seems likely that some form of oblique resonance would have been occurring in these studies. The above results, and the phenomena observed in WP, suggest most strongly that acoustic forcing will readily induce oblique wave resonance.

Observations of oblique wave resonance using imposed two-dimensional wave forcing is shown clearly in §3. Exploration of the smoke wire location proves that these oblique wave observations are not simply an artifact of the smoke visualization technique. Measurements of wake response are presented in §4, followed by an investigation, in §5, into higher-order modes of oblique wave resonance, corresponding to combination frequencies ($f_K - nf_T$). The downstream development of oblique waves is studied in §6, where we investigate the effects of amplitude level on the rise and fall of different modes downstream, for specifically chosen frequencies. Comparisons with predictions based on stability analysis and further discussion are contained in §7, followed by some conclusions in §8.

2. Experimental details

Measurements of velocity fluctuations and spectra using a hot wire, and smoke-wire flow visualization, were made in the same manner as conducted in WP. Throughout this study, the Reynolds number is 150. For the acoustic forcing experiments, we placed a 12 in. Sub-woofer 120 W speaker at the large contoured inlet to the wind tunnel, as shown in figure 3. This was driven by a 75 W audio amplifier, which was controlled by a function generator, from which the amplitude and frequency were varied. The imposed frequency (f_T) was monitored in the test section free stream, using our hot wire coupled to a digital spectrum analyser. The cylinders were constructed of hypodermic tubing of diameters 0.108 and 0.216 cm. It should be noted that the small 'muffin' fan, which produced a very small peak in the free-stream spectrum in WP, and was the cause of our discovery of this phenomenon, was removed for all the present experiments.

The imposed frequency (f_T) is normalized with respect to the Kármán shedding frequency (f_K), as shown below. The amplitude of the imposed two-dimensional wave is defined as the normalized r.m.s. streamwise velocity fluctuation at the frequency f_T (measured in the free stream) observed from the spectrum analyser:

normalized frequency $F = f_T/f_K$;

normalized amplitude $A = (u'_{rms}/U)_{f_T}$.

The origin of the wake coordinate system is fixed on the axis of the cylinder. The x-axis is downstream (defined as streamwise), the y-axis is perpendicular (defined as transverse) to the flow direction and to the cylinder axis, and the z-axis lies along the axis of the cylinder (defined as spanwise). The diameter of the cylinder is denoted D.

3. Observations of oblique wave resonance

One of the first experiments to be conducted using the acoustic forcing involved the case when the oblique resonance wave frequency ($f_{\theta 1}$) was equal to the two-dimensional wave frequency, i.e. $f_{\theta 1} = (f_K - f_T) = f_T$, or in terms of the normalized frequency, $F = 0.50$. This case was thought to be particularly interesting since one might argue from linear theory, in particular Squire's (1933) theorem that, with no

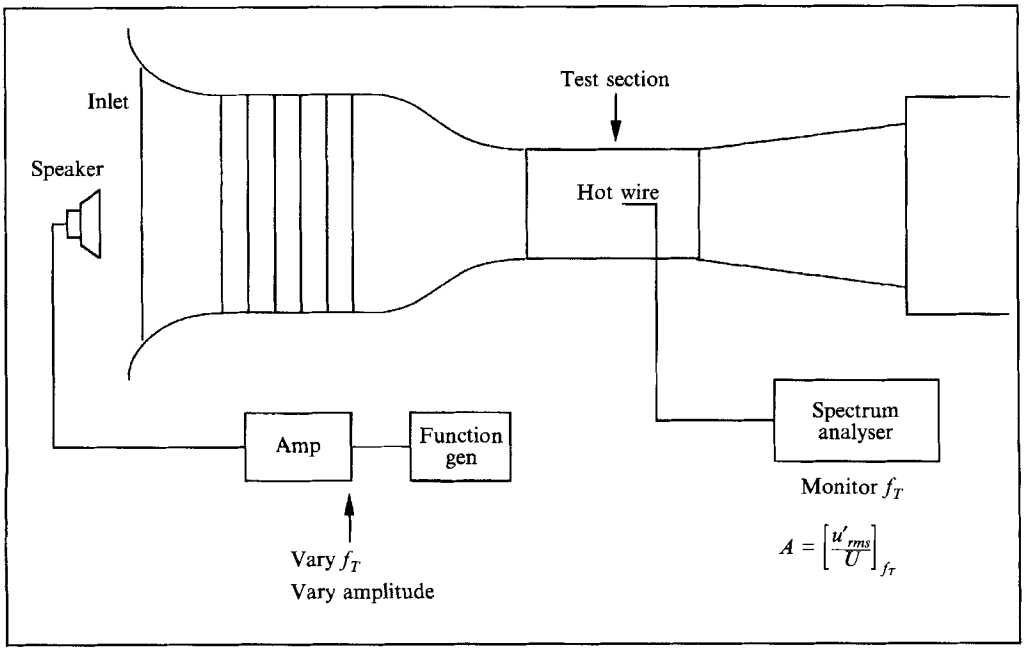

FIGURE 3. Acoustic forcing experimental arrangement.

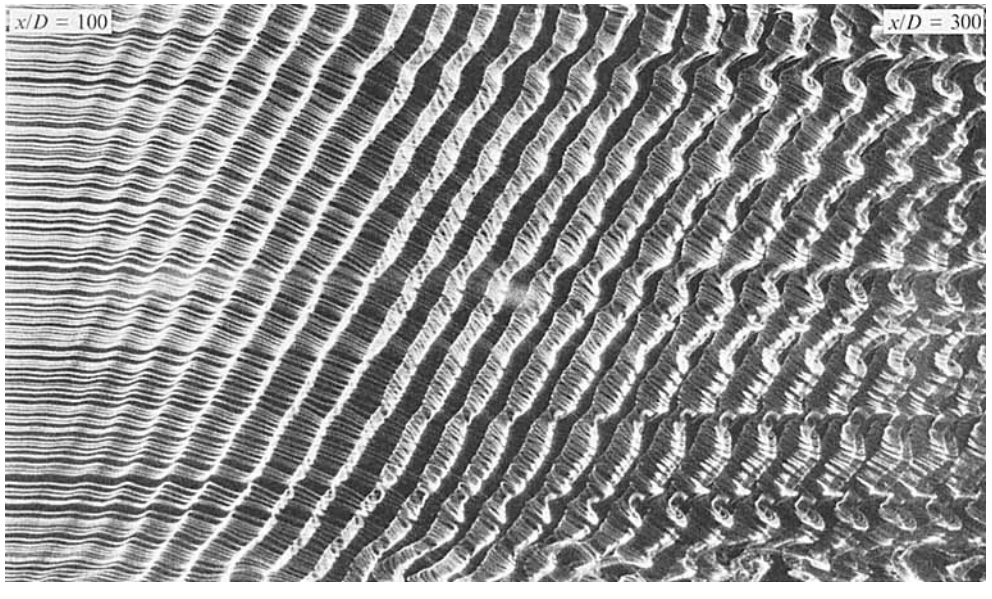

FIGURE 4. Oblique wave resonance for $F = 0.5$: preferential amplification of oblique waves. This visualization demonstrates that, even when the secondary oblique and two-dimensional waves have the same frequency, the oblique waves are preferentially amplified. The smoke wire is placed at $x/D = 100$.

preference for one wave or the other on the basis of the frequency alone, the two-dimensional wave would have the largest growth rate. Certainly it is not possible to separate the frequencies on the spectrum analyser, so the only way to discover which wave is most amplified is to visualize the flow. The visualization of figure 4 shows very

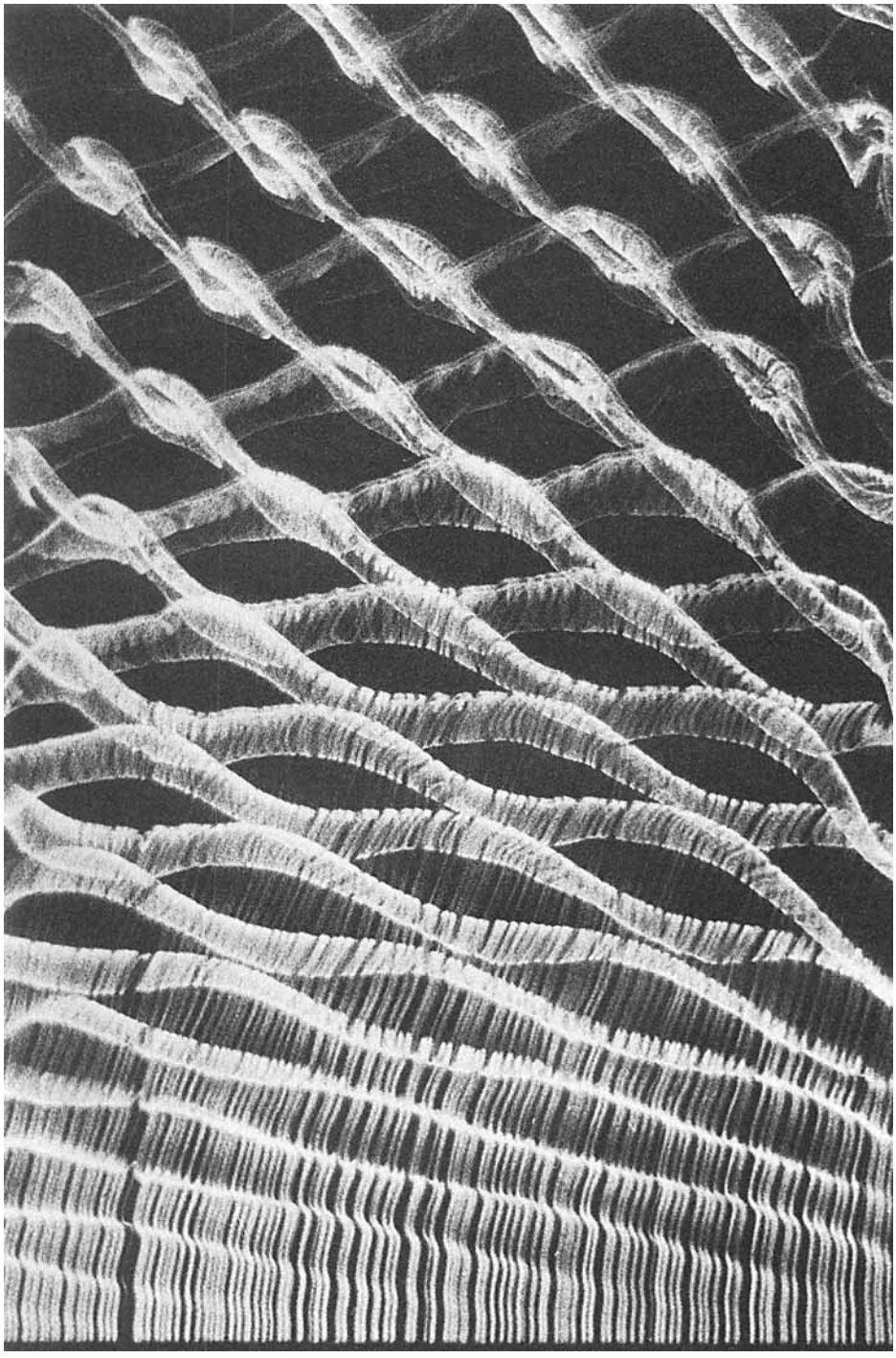

FIGURE 5. Observations of forced wave interactions leading to oblique wave resonance. In this close-up photograph, one can observe at the left, the oblique shedding waves. These waves interact with the two-dimensional waves, in the middle of the picture, to produce the large-angle oblique waves at the right of the picture.

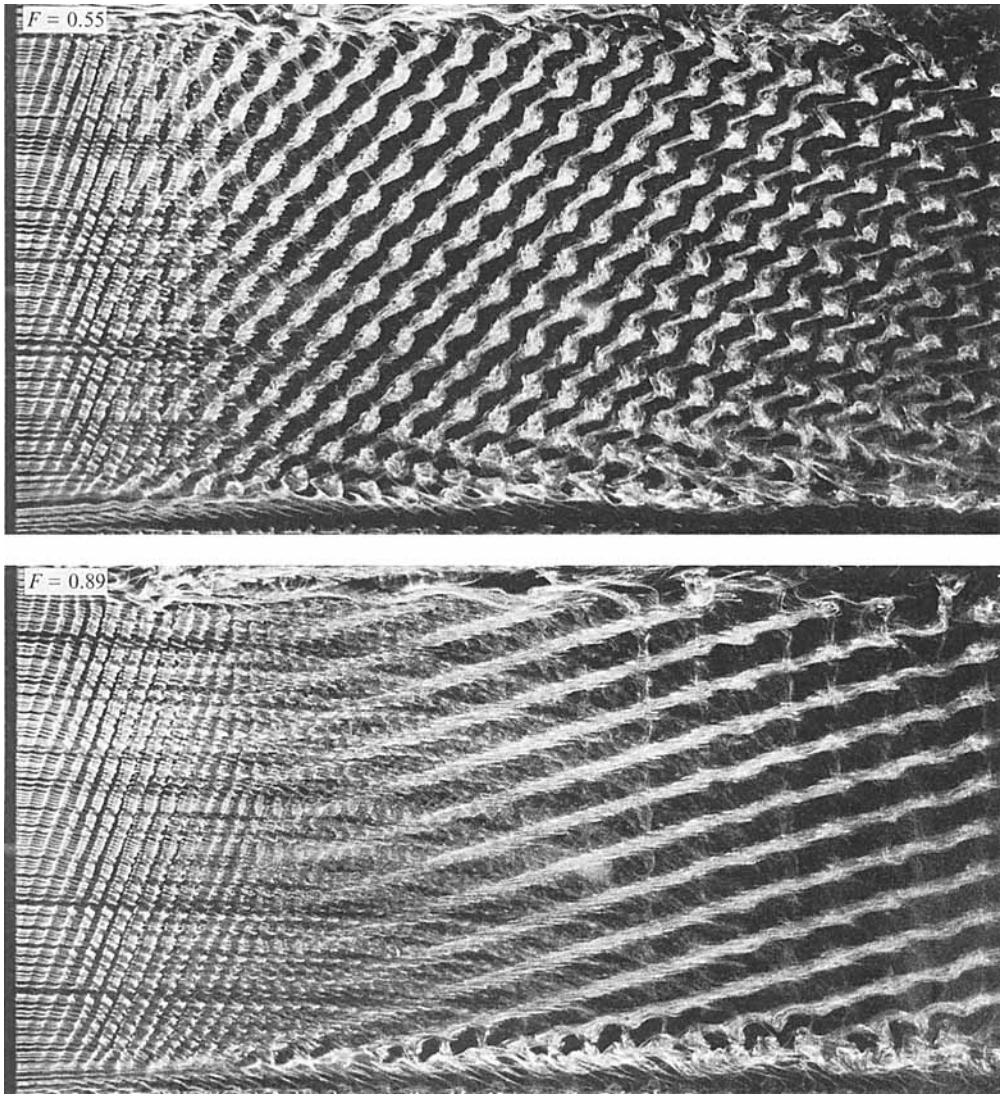

FIGURE 6. Variation of oblique wave angle with frequency ratio F. (*a*) $F = 0.55$, $A = 0.0012$; (*b*) $F = 0.89$, $A = 0.004$. The smoke wire is at $x/D = 50$, and the downstream end of the picture is at $x/D = 300$. The increase in oblique wave angle (up to $\theta_1 = 74°$ in *b*) is caused by an increase in forcing frequency. However, the oblique shedding waves (at the left) are similar in both cases.

clearly that it is the oblique resonance waves that are preferentially amplified; indeed there is very little evidence of the imposed two-dimensional wave. One may note that in this picture the normalized r.m.s. amplitude of forcing is only 0.0004 so that, in accordance with WP, only a very small spectral peak is necessary to trigger resonance.

A close-up photograph of the development of the oblique resonance is shown in figure 5, using the 0.216 cm diameter cylinder. At the left, one may observe the oblique shedding waves, which are deformed by the two-dimensional waves into a wavy form. Segments of each of the deformed oblique shedding waves realign themselves along the lines of the forming oblique resonance waves until, at the right of the picture, the main structure has become these new large-scale oblique waves. The other segments of each

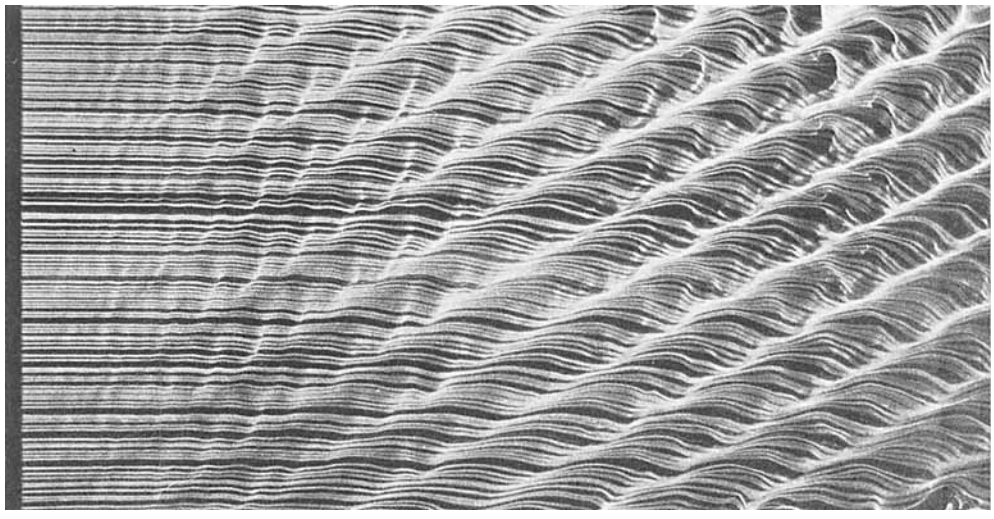

FIGURE 7. Visualization downstream of large-angle 64° oblique waves, for $F = 0.84$. The smoke wire is at $x/D = 100$, and the right side of the picture is at $x/D = 300$. $A = 0.004$.

oblique shedding wave are stretched into a direction normal to the oblique resonance waves. This deformation and the apparent interlinking between the waves has an appearance similar to the preliminary computations of imposed oblique waves on a planar wake carried out very recently by Meiburg (1992).

The effect of different forcing frequencies on the geometry of the oblique wave pattern is shown in figure 6. It may be deduced from the equations of the interacting waves (for example, (14) and (15) in WP) that the oblique wave angle (θ_1) increases as the normalized frequency (F) increases

$$\tan\theta_1 = \frac{\tan\theta_K}{1-F}, \tag{1}$$

where θ_K is the oblique shedding angle. (This relationship is plotted later as part of figure 14.) This trend is clearly seen in the photographs of figure 6, where the oblique resonance wave takes the angle $\theta_1 = 43°$ for $F = 0.55$, and a remarkable $\theta_1 = 74°$ for $F = 0.89$, and these waves may be compared with the original oblique shedding vortices at the left of the pictures. Much attention has been paid in the past to subharmonic resonances in shear flows, and it is perhaps initially surprising that oblique resonance will occur for such a high frequency ratio F, which is far removed from the subharmonic frequency case. In figure 7, where the smoke wire has been placed further downstream at $x/D = 100$, such large-angle waves for $F = 0.84$ ($\theta_1 = 64°$) are seen to develop as the principal waves at these downstream locations. It was confirmed here that oblique waves were not simply an artifact of the visualization technique, by placing the smoke wire at various different downstream positions, and also at different lateral positions (as done in WP).

4. Measurements of wake response

Here, the wake response is found at a particular downstream location $x/D = 150$, which was previously found (in WP) to be a position near the saturation amplitude for a secondary wake. Obviously, one could choose other positions to characterize wake

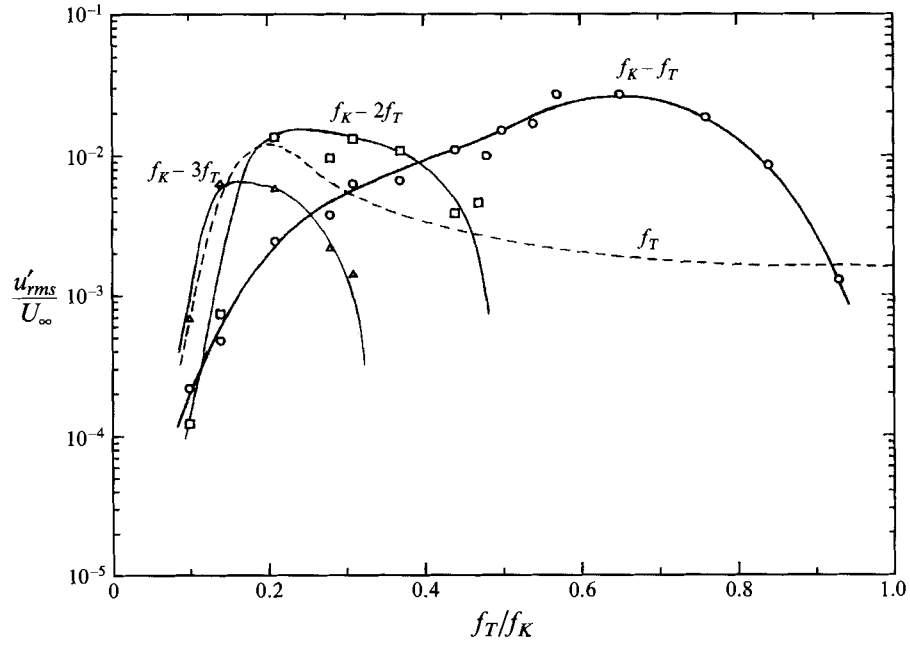

FIGURE 8. The responses of the different oblique resonance modes $(f_K - f_T)$, $(f_K - 2f_T)$, $(f_K - 3f_T)$ over a range of F are shown, along with the response of the two-dimensional wave mode (f_T). An estimate of the normalized frequency for peak response of the oblique modes is $F = \frac{1}{2}, \frac{1}{4}, \frac{1}{6}, \ldots$ respectively. In this plot, $A = 0.002$.

response and therefore, in §6, we will investigate how the response is a function of downstream location for specifically chosen frequency ratios, F. In the sections that follow, the oblique vortex shedding angle is fixed (by controlling the spanwise end boundary conditions of the cylinder) such that $\theta = 14°$ or $15°$.

A measure of the wake response, over a range of F and for a constant amplitude, $A = 0.002$, is given in figure 8. (Other forcing amplitudes were investigated and, although some differences were found, the general character is well exhibited here.) It can be seen that the peak response is found for the particular combination frequency $(f_K - f_T)$ that has been discussed in detail above, at approximately the forcing frequency $F = 0.55$–0.6. However, we have plotted the response of all the principal modes which appear in the far-wake frequency spectra. 'Higher-order' modes such as $(f_K - 2f_T)$ and $(f_K - 3f_T)$ appear to exhibit peak responses at lower F. For $F < \frac{1}{2}$, the mode $(f_K - 2f_T)$ has a peak resonance at around $F = \frac{1}{4}$, while for $F < \frac{1}{3}$, the mode $(f_K - 3f_T)$ has a peak resonance at around $F = \frac{1}{6}$. The two-dimensional waves themselves seem to reach a peak also at around $F = 0.2$. It should still be noted that these data only represent the measurements at $x/D = 150$, and there is some development in the modes as one travels downstream.

Following this presentation, on might question what actual far-wake frequencies are most amplified, irrespective of the modes (e.g. $(f_K - f_T)$, $(f_K - 2f_T)$, ...) they represent. For this purpose, these frequencies are normalized by the Kármán frequency (f_K), and their response curves are plotted in figure 9. Consistent with the earlier plot, the first oblique mode $(f_K - f_T)$ has a broad peak response when $(f_K - f_T)/f_K = 0.4$–0.45. The second mode $(f_K - 2f_T)$ also has a broad peak response when its frequency is $(f_K - 2f_T)/f_K = 0.4$–0.45, and similarly for the third mode $(f_K - 3f_T)$. The data show

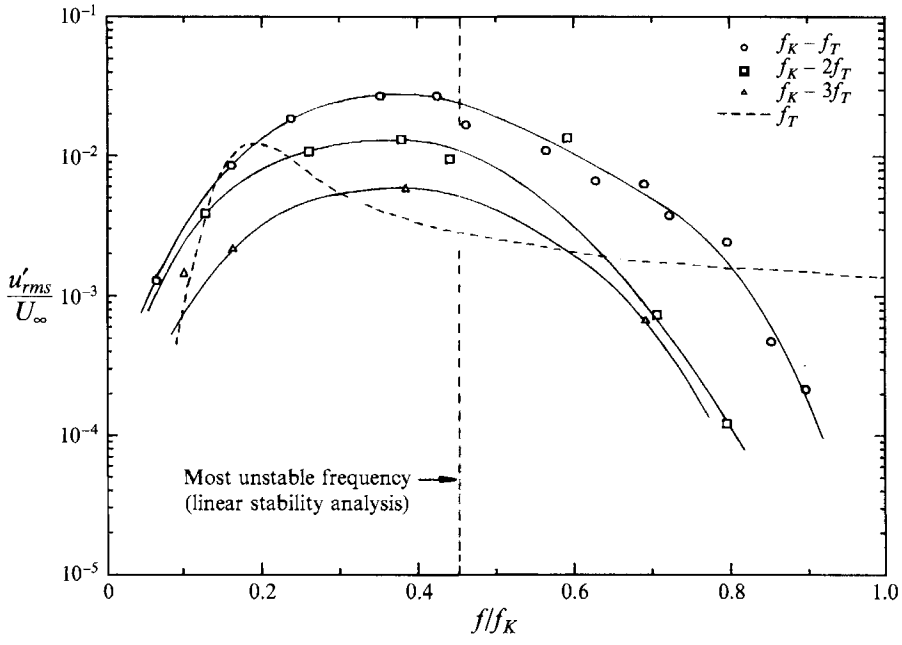

FIGURE 9. Response of higher-order oblique modes versus far-wake frequency. Experimental measurements show that the actual frequency of peak response for all the oblique modes is centred around 0.4–0.45 of the shedding frequency. The most unstable frequency adapted from analysis (of Cimbala *et al.* 1988) is 0.457 of the shedding frequency evaluated locally at $x/D = 150$, $Re = 150$.

that all the combination-frequency modes have a peak response when their actual frequency is around 0.4–0.45 of the Kármán shedding frequency, but that the response diminishes as the order of the mode increases.

This value for the peak response frequency is close to what may be predicted using the linear spatial inviscid stability analysis carried out by Cimbala *et al.* (1986), as calculated for the mean wake profile at $Re = 150$ and $x/D = 150$. The frequency for maximum growth rate is found using the curves of growth rate versus normalized frequency $\beta = 2\pi\delta f/U_\infty$ in figure 12 of Cimbala *et al.*, which are a function of the normalized defect velocity W_0/U_∞. (In the above expression, δ is the wake half-width for a Gaussian mean velocity profile, and U_∞ is the free-stream velocity.) For our case, from figure 26 of WP, $W_0/U_\infty = 0.20$ and the normalized wake half-width $(\delta/D) = 1.4$. This gives, from Cimbala *et al.* a most-unstable frequency defined by $\beta = 0.74$, and with the Strouhal frequency $(S_K) = 0.1839$, we obtain a normalized frequency for maximum growth rate as

$$\frac{f}{f_K} = \frac{\beta}{2\pi}\frac{1}{\delta/D}\frac{1}{S_K} = 0.457, \tag{2}$$

which is in the vicinity of the broad peak response found experimentally at $(f/f_K) = 0.4$–0.45. (It should be noted that the predicted frequency is only locally valid.)

One can observe from figure 8 that the oblique mode $(f_K - f_T)$ has roughly an amplitude a factor of 10 greater than the two-dimensional waves (f_T), in the vicinity of $F = 0.5$, i.e. the case when the oblique and two-dimensional waves have the same frequency. It is not possible to find from the spectra which of these waves is most amplified at exactly $F = 0.5$, so in order to support the observations of oblique waves

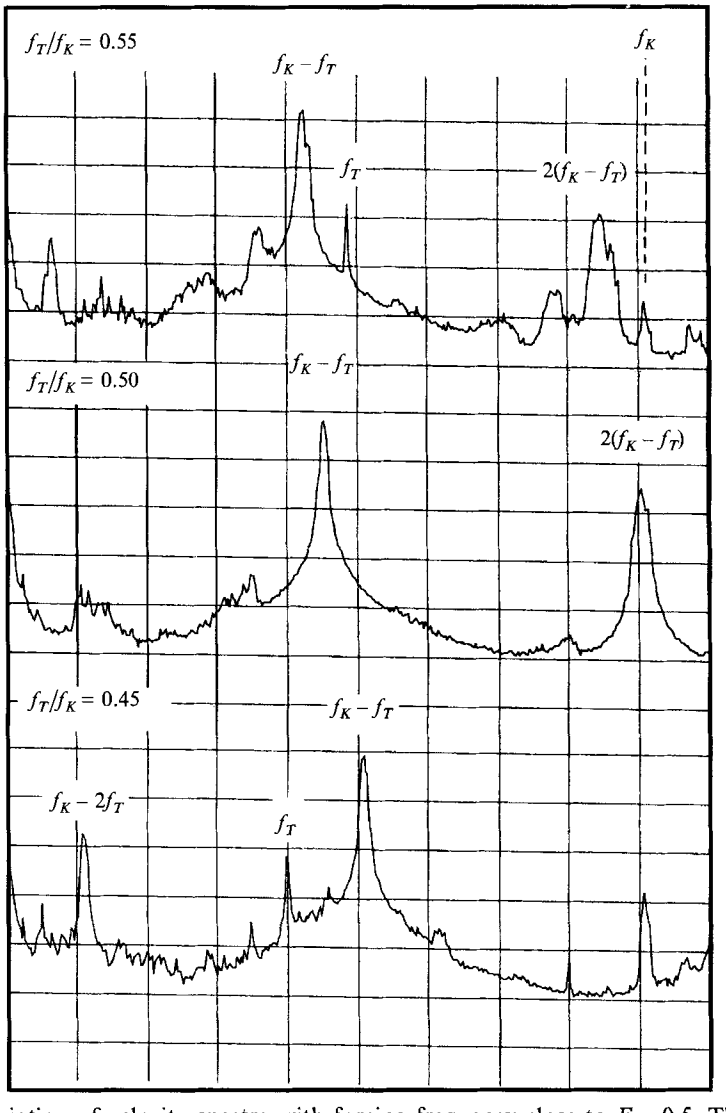

FIGURE 10. Variation of velocity spectra with forcing frequency close to $F = 0.5$. The normalized frequency F is reduced in steps through the $F = 0.5$ case, showing the preferential amplification of the oblique wave frequency $(f_K - f_T)$ close to $F = 0.5$. In this case, $A = 0.0012$, $x/D = 150$, and the vertical scale is 10 dBV/div.

presented earlier in figure 4, we have decreased the imposed frequency F in small steps from just above $F = 0.5$ to just below $F = 0.5$. In the spectra of figure 10, the energy for the oblique waves at frequency $(f_K - f_T)$ is clearly greater than for the two-dimensional waves (f_T) when F is just greater than 0.5. There is then a single large peak under the conditions when $F = 0.50$, and for F just below 0.5, again the oblique waves have far more energy than the two-dimensional waves. Although one cannot prove without visualization or two-point measurements that the oblique waves are most amplified when their frequency is the same as that of the two-dimensional waves, it is clear that their energy is much higher as one progresses the frequency through $F = 0.5$.

5. Higher-order modes of oblique wave resonance

In this Section, we shall be concerned principally with observations and measurements of higher-order oblique wave resonances which have frequencies $(f_K - nf_T)$, where n is an integer.

In the lower spectrum of figure 10, for which $F = 0.45$ (i.e. $F < 0.50$), one can see that the higher oblique resonance frequency $(f_K - 2f_T)$ can now be seen. For still lower values of F, the spectra contain more peaks for the different oblique modes, and an example is shown in figure 11, for $F = 0.31$. In this case, F lies in the range $\frac{1}{4}$ to $\frac{1}{3}$, so one can observe frequency peaks corresponding to $(f_K - f_T)$, $(f_K - 2f_K)$ and $(f_K - 3f_T)$. The fact that there is energy at such combination frequencies suggests that they represent waves that should be observed in the same manner as the oblique waves for $(f_K - f_T)$. We shall here extend consideration of wave interactions, discussed in WP, to the case of the higher-order combination frequencies, each of which interacts with the two-dimensional waves. If, instead of f_K interacting with f_T, we have $(f_K - (n\text{-}1)f_T)$ interacting with f_T, then general expressions for the geometry of the resonance waves may be written, following a similar approach to that used in WP. Alternatively, the higher-order modes may be interpreted in terms of an interaction between the following waves:

$$a_K e^{i(\boldsymbol{k}_K \cdot \boldsymbol{x} - \omega_K t)},$$
$$a_T e^{in(\boldsymbol{k}_T \cdot \boldsymbol{x} - \omega_T t)},$$

giving an equation for the resonance wave in the wavenumber space as

$$\boldsymbol{k}_{\theta n} = \boldsymbol{k}_K - n\boldsymbol{k}_T. \tag{3}$$

Equations (4)–(7) below may be deduced from simple geometrical inspection of the wavenumber diagram shown in figure 12. In the following, note that the wavelengths $\lambda_{\theta n}$, λ_K and λ_T are the streamwise wavelengths for the resonance wave, the oblique shedding wave and the two-dimensional wave respectively, whereas λ_{Zn} and λ_{ZK} denote spanwise wavelengths (in the z-direction).

Frequency of nth oblique wave, $f_{\theta n}$

$$f_{\theta n} = f_K - nf_T; \tag{4}$$

spanwise wavelength of nth oblique wave, λ_{Zn}

$$\lambda_{Zn} = \lambda_{ZK}; \tag{5}$$

streamwise wavelength of nth oblique wave, $\lambda_{\theta n}$

$$\frac{\lambda_{\theta n}}{\lambda_K} = \frac{\lambda_T/\lambda_K}{\lambda_T/\lambda_K - n}; \tag{6}$$

angle of nth oblique wave, θ_n

$$\frac{\tan\theta_n}{\tan\theta_K} = \frac{\lambda_{\theta n}}{\lambda_K}. \tag{7}$$

The equations above for the first oblique resonance mode $(f_K - f_T)$ define oblique waves which pass through the nodes formed by the superposition of the oblique shedding waves (f_K) and the two-dimensional waves (f_T). This is shown diagramatically on the left part of figure 13, where the solid lines on the left represent the first oblique resonance waves passing through the nodes of the other two wave systems (shown as dashed lines). As the flow travels downstream to the right, so the wake instability tends to amplify lower frequencies. One such lower frequency, shown in this figure, is the

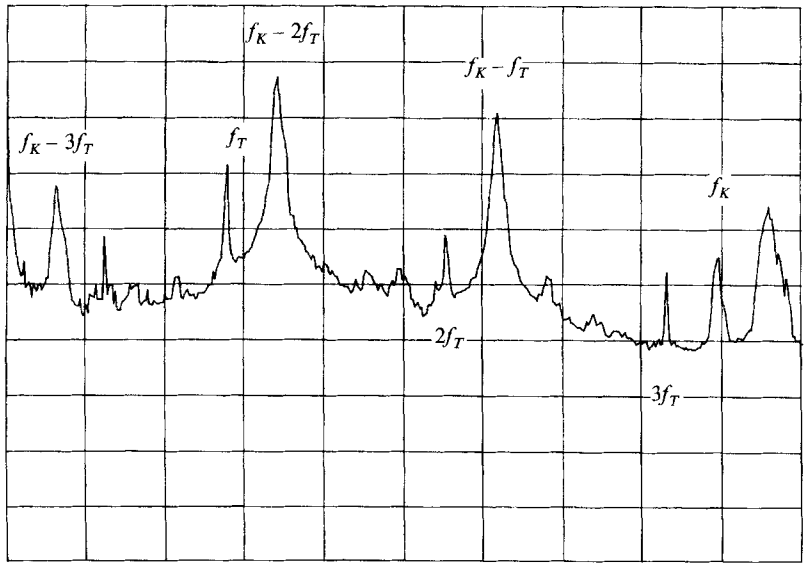

FIGURE 11. Velocity spectrum for $F = 0.31$. In this case peaks corresponding to three oblique modes and the two-dimensional mode may be seen. At this location, $x/D = 150$, the second oblique mode $(f_K - 2f_T)$ is taking over from the first mode $(f_K - f_T)$ as the wake travels downstream, and the lower frequencies become amplified. $A = 0.002$, vertical scale is 10 dBV/div.

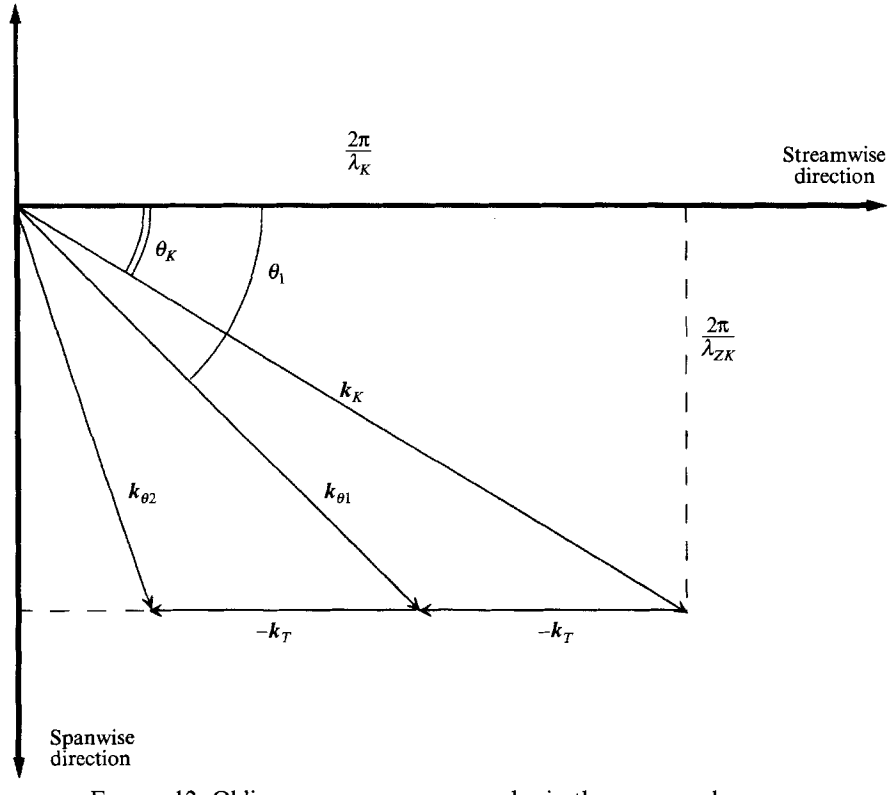

FIGURE 12. Oblique wave resonance modes in the wavenumber space.

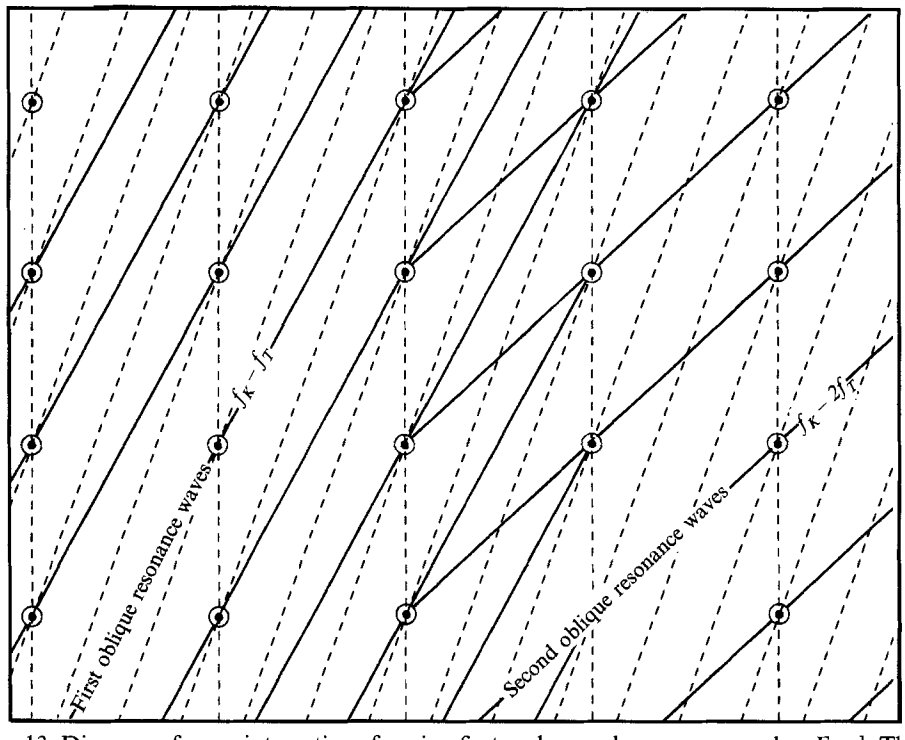

FIGURE 13. Diagram of wave interactions forming first and second resonance modes, $F = \frac{1}{3}$. The first oblique resonance waves $(f_K - f_T)$ (solid lines) pass through the nodes formed by the superposition of the oblique shedding waves and the two-dimensional waves (both dashed lines). A larger wavelength second oblique resonance $(f_K - 2f_T)$ occurs further downstream (to the right), and again these waves pass through nodes of the same superposition pattern but, in the latter case, at a larger angle.

second mode $(f_K - 2f_T)$, which is caused by the interaction of the first oblique waves $(f_K - f_T)$ with the two-dimensional waves (f_T). As for the first mode, we can now interpret the lines for the mode $(f_K - 2f_T)$ as passing through the nodes formed by the superposition of the oblique waves $(f_K - f_T)$ with the two-dimensional waves (f_T). Similar conclusions are drawn for the nth mode, and indeed these geometrical interpretations follow directly from (3).

One can therefore envisage a sequence of resonances occurring as the wake travels downstream, as follows:

$$\begin{aligned}
&\text{1st oblique resonance} && (f_K) \xrightarrow[\Downarrow]{\text{interaction}} (f_T)\\
&\text{2nd oblique resonance} && (f_K - f_T) \xrightarrow[\Downarrow]{\text{interaction}} (f_T)\\
&\text{3rd oblique resonance} && (f_K - 2f_T) \xrightarrow[\Downarrow]{\text{interaction}} (f_T).
\end{aligned}$$

This sequence may occur so long as the normalized facing frequency makes the relevant oblique resonance frequencies non-negative, for example $(f_K - 2f_T)$ only occurs for $F < \frac{1}{2}$ or, more generally, the nth oblique resonance mode may only occur when the following simple inequality holds:

$$F < 1/n. \tag{8}$$

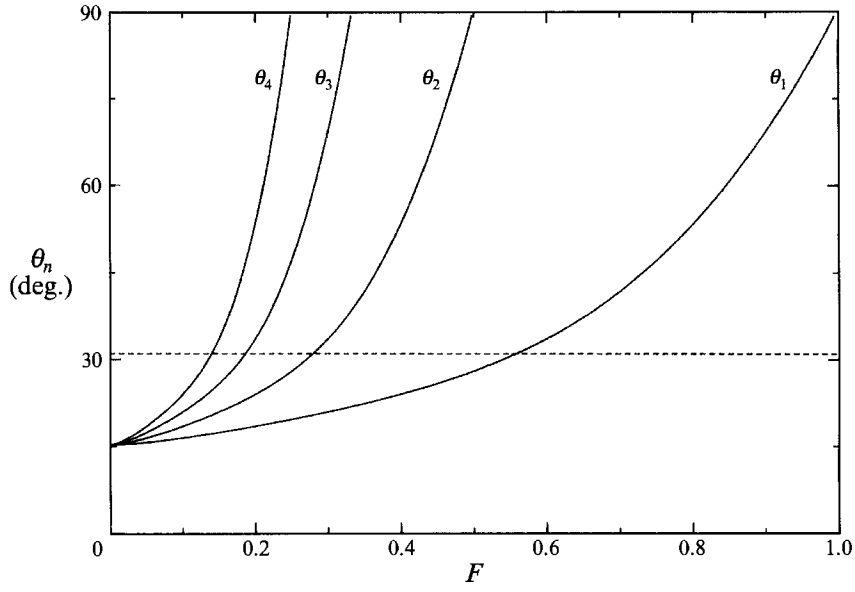

FIGURE 14. Oblique wave angles for higher oblique modes, plotted from equation (9), versus forcing frequency F. The horizontal line marks the angle of peak response, 31° (for an oblique shedding angle of 15°). The intersections with the oblique-angle curves give the values of F for peak response.

Other geometric characteristics of the flow are demonstrated simply from (4)–(7). Clearly, the spanwise wavelengths for all the oblique wave systems must be the same, and all are equal to the spanwise wavelength of the oblique shedding waves. The oblique resonance wave angles (relative to the two-dimensional wave) are given by (7), or, on the assumption that the waves are locked in phase speed,

$$\tan\theta_n = \frac{\tan\theta_K}{1-nF}. \tag{9}$$

This straightforward relation is shown for the different oblique resonance modes in figure 14, for the case where the oblique shedding angle is a constant, $\theta_K = 15°$. If we use the condition that in these experiments, the maximum oblique wave response is found when $(f/f_K) = 0.45$ (evaluated at the position downstream where typically the first mode of the secondary wake reaches a saturation amplitude), then for the nth oblique resonance mode, $nF = 0.55$. Substituting this into (9), one finds that the angle for maximum response is $\theta_n = 31°$, and this is plotted as the horizontal dashed line in figure 14. For each of the oblique modes, the intersection of this dashed line with each of the θ_n curves gives the value of F where a peak response is expected. The oblique shedding angle of 15° used in these calculations is perhaps typical of many of the cylinder wake experiments, and therefore a large response for an oblique wave angle near 31° would probably be typical in different facilities, for a Reynolds number of around 140–160.

For a more approximate but useful estimate of the normalized frequencies where a peak response is expected, one can take the maximum response to be $nF = 0.5$ (this is a not unreasonable estimate given that the response has a broad peak), so that

frequency for maximum wake response

$$F_{max} = \frac{1}{2n} = \tfrac{1}{2}, \tfrac{1}{4}, \tfrac{1}{6}\ldots. \tag{10}$$

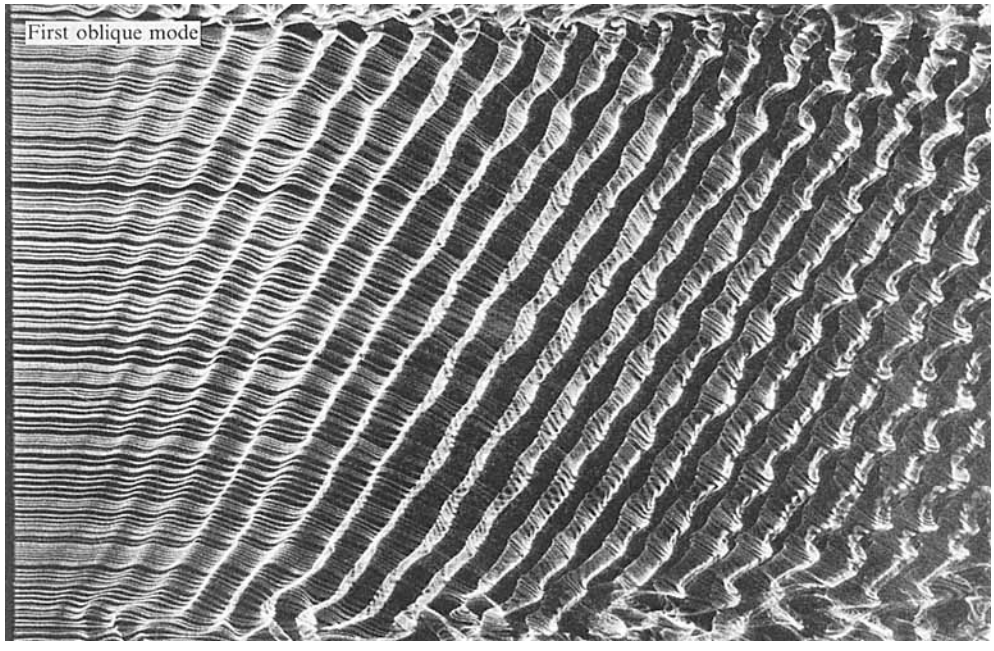

FIGURE 15. Wave angles for maximum response, first oblique mode. $F = 0.55$, $x/D = 100$ to 300, and $A = 0.0004$. $\theta_1 = 32°$.

Also, from (9), an estimate of the oblique wave angle for peak response would be given by $\tan\theta_n = 2\tan\theta_K$, or rather roughly

oblique wave angle for peak response

$$\theta_{max} = 2\theta_K. \tag{11}$$

Visualization of the first oblique resonance mode ($f_K - f_T$) for the condition of peak response is shown in figure 15, corresponding to a normalized frequency $F = 0.55$, and to an angle $\theta_1 = 32°$. In this case the smoke is introduced at $x/D = 100$. Similarly, for the second oblique resonance mode ($f_K - 2f_T$) in figure 16, maximum response is found for a normalized frequency of $F = 0.28$, and the waves in this case have an angle of 33°, in agreement with the simple geometric considerations above. The smoke in this figure was also introduced at $x/D = 100$, and the waves at the left of the picture are the first oblique resonance waves (not to be confused with the oblique shedding waves). In accordance with the sequential scenario suggested above, the first oblique mode interacts with parallel waves at the left of the picture to deliver the second oblique resonance waves at the right.

In order to show that the second oblique resonance waves are not simply some artifact of visualization, a smaller cylinder was placed in the tunnel so that photographs could be taken at larger normalized distances downstream. In figure 17, for a frequency $F = 0.287$, the smoke is introduced at $x/D = 200$, and we see the second oblique resonance waves form as the principal waves, down to $x/D = 510$.

6. Downstream development of oblique waves

The measurements to this point give an overall characterization of the wake response. The response is evaluated at a location downstream where, approximately,

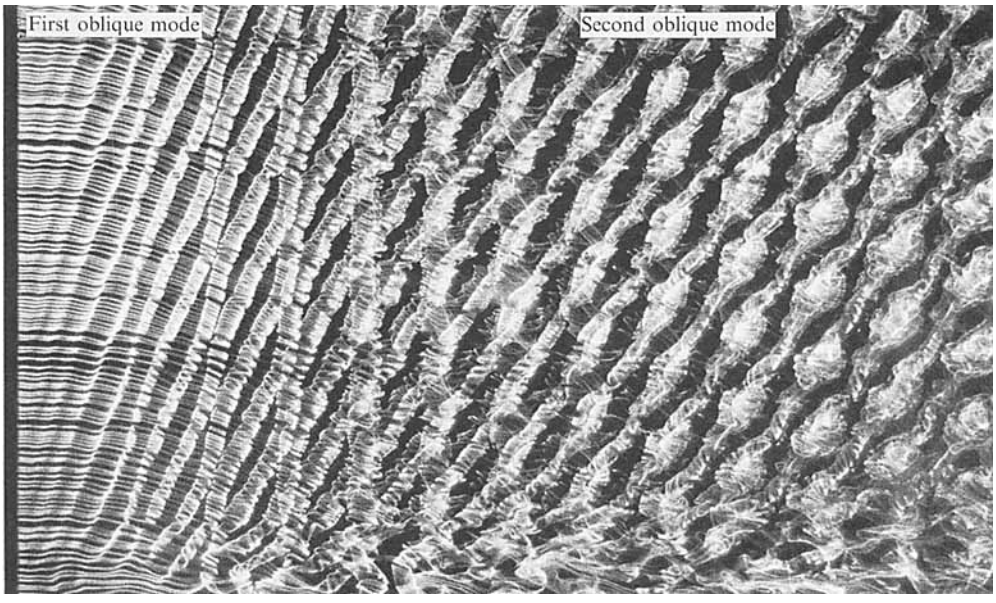

FIGURE 16. Wave angles for maximum response, second oblique mode. $F = 0.28$, $x/D = 100$ to 300, and $A = 0.002$. $\theta_2 = 33°$.

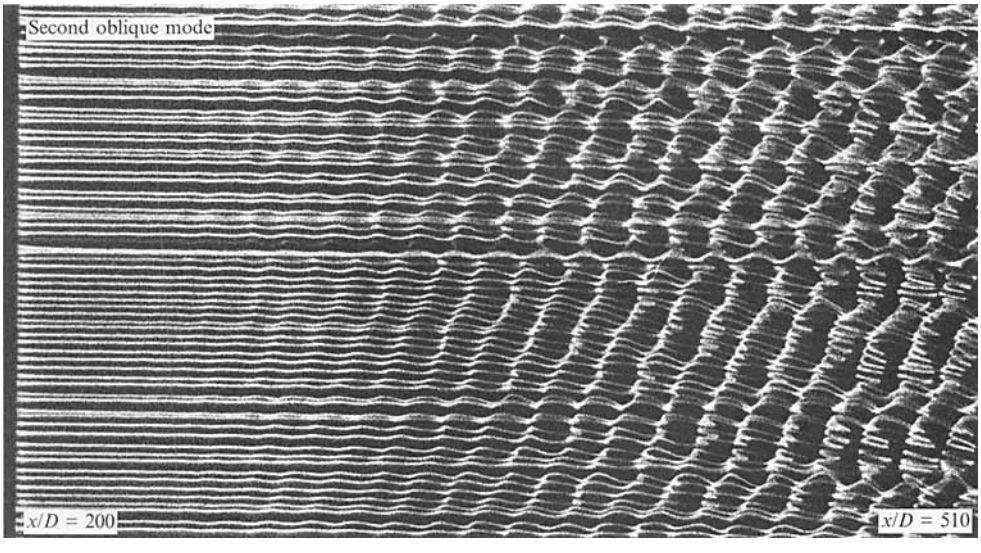

FIGURE 17. Observations of second oblique mode far downstream (for small cylinder). $F = 0.287$, $A = 0.002$.

the first of the secondary modes will have reached a saturation amplitude. However, different amplified oblique or parallel modes may appear in different ranges of downstream distance.

In WP, it was shown that when $F > 0.5$, then there exists an 'Oblique' mode, for which the wake exhibited an oblique resonance ($f_K - f_T$) at all downstream locations studied. In this case, we found that the two-dimensional mode (f_T) has a frequency that is above the first oblique mode ($f_K - f_T$), and thereby does not become amplified

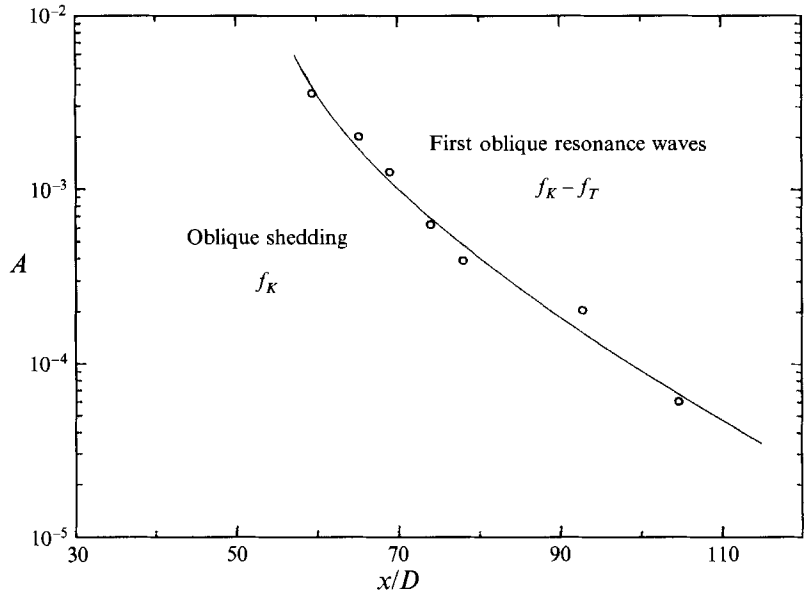

FIGURE 18. Regions of oblique shedding waves and first oblique mode in the (x, A)-plane, $F = 0.55$. The data are taken at the downstream position at which the decaying energy at the oblique shedding frequency (f_K) is equal to the growing energy at the frequency of the first oblique mode ($f_K - f_T$).

further downstream, because the wake responds more to lower frequencies. When $F < 0.5$, we observed an 'Oblique–Two-dimensional' mode, whereby the oblique mode ($f_K - f_T$) is amplified first, followed further downstream by the two-dimensional mode (whose frequency is lower and more amplified downstream than the oblique mode).

It appears from the present work that there are indeed other possibilities, which are a function of the frequency and amplitude of the two-dimensional wave forcing. There is the possibility for second and third oblique wave resonances to occur, depending on the value of F. In WP, we studied the case (for $Re = 150$) where F was slightly less than 0.5, demonstrating the Oblique–Two-dimensional mode. In this paper, we shall specifically investigate two main cases, also for $Re = 150$, which are F just greater than 0.5 ($F = 0.55$), and F low enough so that ($f_K - 2f_T$) exists in the flow ($F = 0.36$).

In the case $F = 0.55$, over the range of amplitudes A plotted in figure 18, we find that the oblique shedding waves give way to the first oblique mode ($f_K - f_T$) at a certain distance downstream, which varies with the amplitude. This distance in figure 18 is defined at the point where the decaying energy of the oblique shedding waves is equal to the growing energy of the secondary mode (defined as the start of the 'far wake' in figure 16 of WP). As A is increased, the interactions leading to oblique resonance occur further upstream, and correspondingly the energy in the interactions is stronger, since both the oblique shedding waves and the two-dimensional forcing waves are at a higher amplitude. The surprising conclusion is that the higher the two-dimensional wave forcing is, the larger is the oblique resonance wave response!

The downstream development of velocity fluctuations for $F = 0.55$ is shown in figure 19. For the imposed forcing amplitude of $A = 0.002$, the oblique resonance waves at ($f_K - f_T$) become the predominant spectral peak at around $x/D = 63$. Thereafter, the oblique waves dominate the far wake, in preference to the two-dimensional waves (f_T).

The case $F = 0.36$ is certainly more complex, involving as it does the far-wake frequencies ($f_K - f_T$), (f_T), and ($f_K - 2f_T$), in descending order of magnitude (their

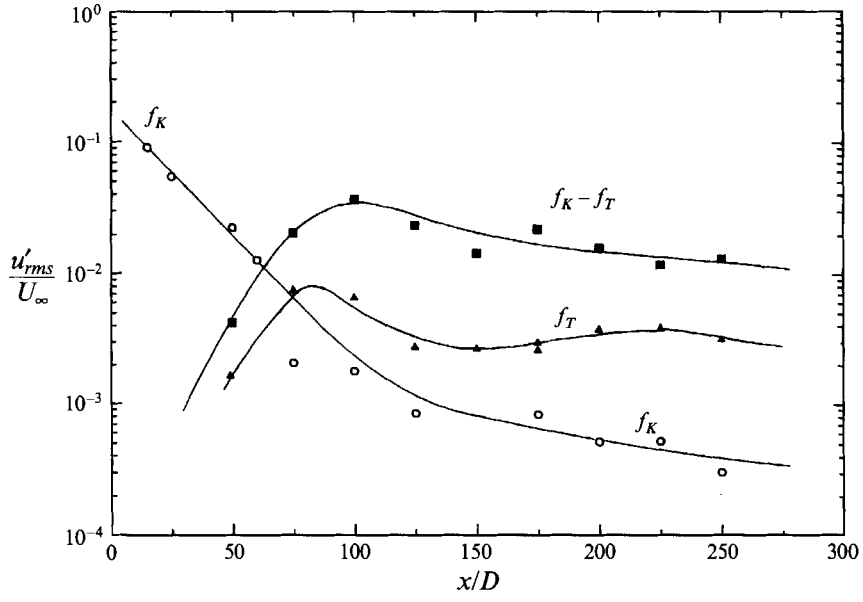

FIGURE 19. Downstream development of velocity fluctuations, $F = 0.55$: the oblique resonance waves are preferentially amplified over the two-dimensional waves at all downstream locations (since the oblique wave frequency is lower than the two-dimensional wave frequency). $A = 0.002$.

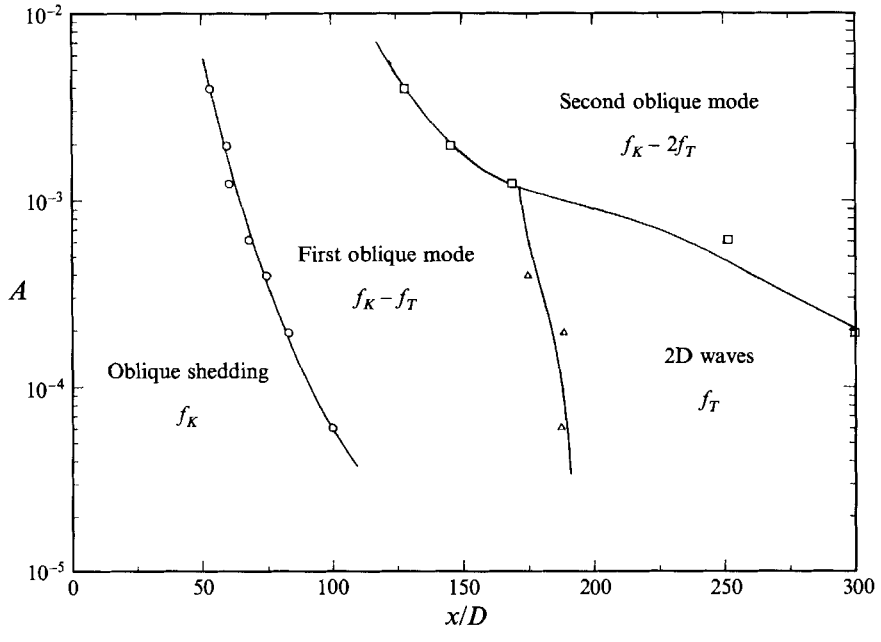

FIGURE 20. Regions of oblique and two-dimensional modes in the (x, A)-plane, $F = 0.36$. These regions, showing the most prominent modes in the (x, A)-plane, are bounded by lines for which the modes to each side have the same energy in the spectra at that particular x/D location.

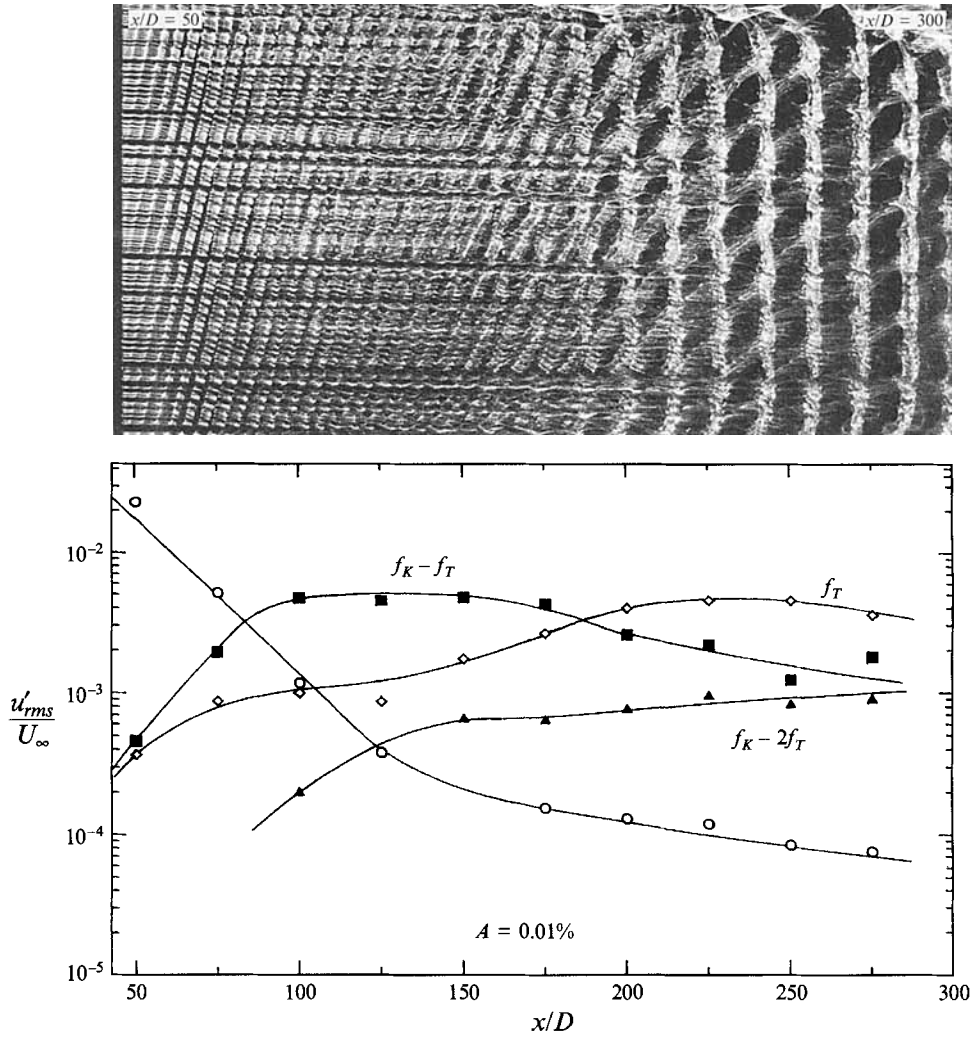

FIGURE 21. Downstream 'low-amplitude' sequence of modes, $A = 0.0001$, $F = 0.36$. The flow visualization corresponds with the fluctuation measurements shown underneath, over the range of $x/D = 50$ to 300.

frequencies, normalized by f_K, are respectively 0.64, 0.36, 0.28). Based on the idea that the far wake will amplify each of these frequencies in turn (in descending order as the wake becomes wider with downstream distance) one might expect the following sequence of most-amplified modes:

low-amplitude sequence

$$f_K \rightarrow (f_K - f_T) \rightarrow (f_T) \rightarrow (f_K - 2f_T).$$

This is indeed the order in which the most-amplified modes appear in the far wake for low amplitudes of forcing, $A < 0.001$, as shown in figure 20. However, for $A > 0.001$, it seems that the wave interactions are more vigorous. The first oblique mode $(f_K - f_T)$ occurs further upstream (like the $F = 0.55$ case), and the second oblique resonance mode also occurs further upstream, such that the flow bypasses altogether the regime where the two-dimensional waves are most amplified, as follows:

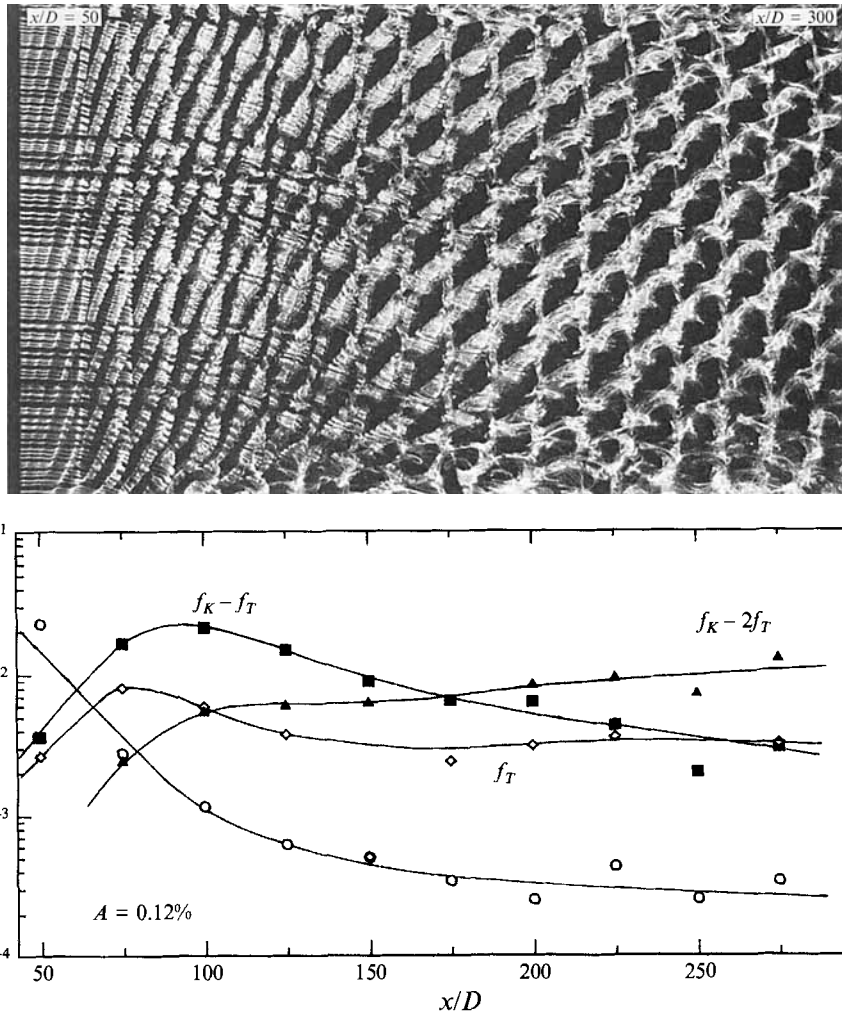

FIGURE 22. Downstream 'high-amplitude' sequence of modes, $A = 0.0012$, $F = 0.36$. As figure 21 but the larger forcing amplitude of the two-dimensional waves paradoxically inhibits the two-dimensional wave response, and preferentially amplifies the second oblique mode.

high-amplitude sequence $f_K \rightarrow (f_K - f_T) \rightarrow \quad \rightarrow \quad \rightarrow (f_K - 2f_T)$.

Development of the spectral amplitudes with downstream distance are shown in figures 21 and 22. In figure 21, for $A = 0.0001$, it may be seen that we follow the low-amplitude sequence above, and the corresponding flow visualization demonstrates the presence of the oblique shedding waves, and the oblique resonance waves, followed by the two-dimensional waves over a certain range of downstream distances. On the other hand, for $A = 0.0012$ (a ten-fold increase), we find that the most-amplified modes follow the high-amplitude sequence, as shown in figure 22. The corresponding flow visualization shows a small portion of oblique shedding waves upstream (at the left), followed by a region of the first oblique mode ($f_K - f_T$), followed by a region (from $x/D = 175$ onwards) where the second oblique resonance waves ($f_K - 2f_T$) are prominent. It should be noted that the flow visualizations in figures 21 and 22 involve

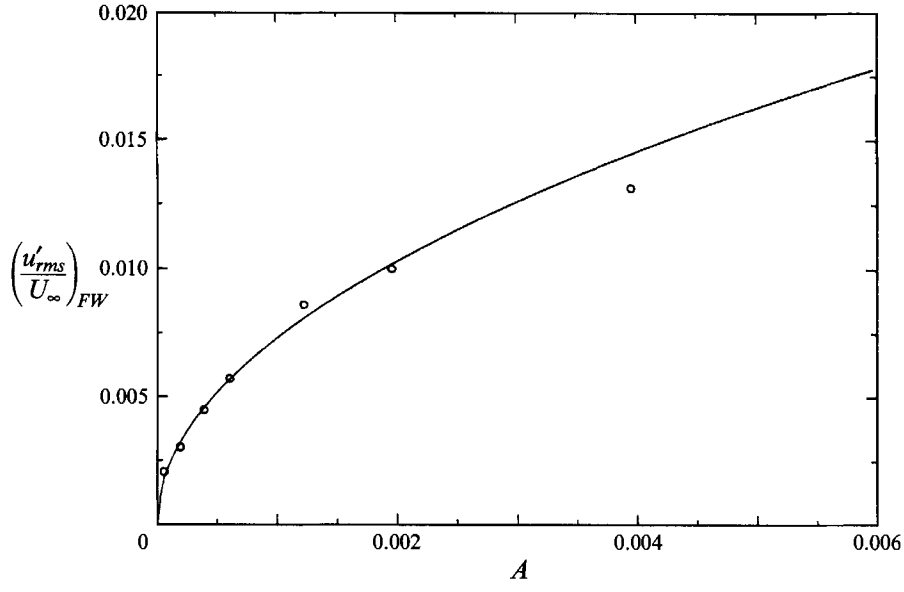

FIGURE 23. Variation of wake response amplitude $(u'_{rms}/U)_{FW}$ with forcing amplitude, A. The wake response follows closely the relationship (solid line) $(u'_{rms}/U)_{FW} = 0.200\,A^{\frac{1}{2}}$.

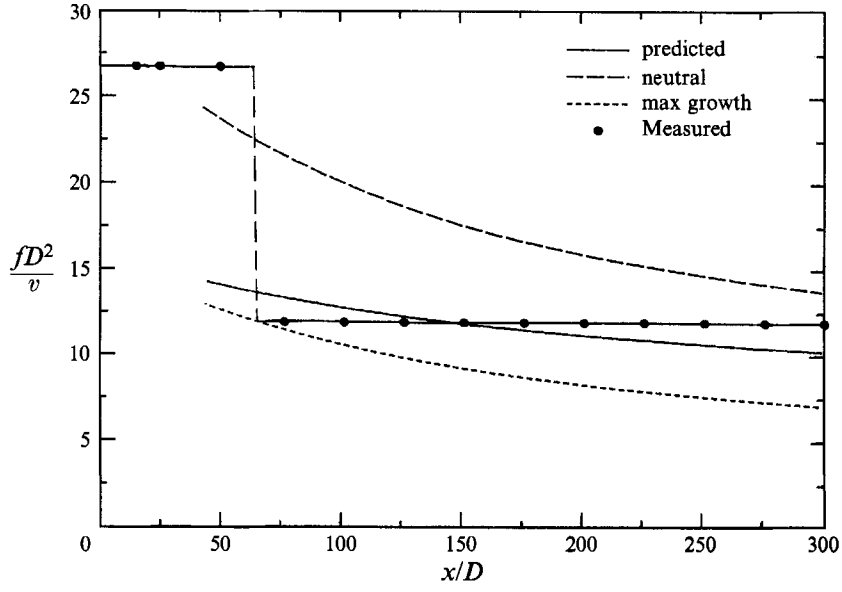

FIGURE 24. Measured and predicted far-wake frequencies versus x/D, $F = 0.55$.

exactly the same experimental arrangement, except for the level of two-dimensional wave forcing amplitude. Again, it is perhaps surprising that, for an increase in two-dimensional wave forcing amplitude, it is the oblique resonance modes that become stronger, indeed to the level where they inhibit the two-dimensional parallel waves from ever being predominant in the wake!

A characteristic wake response amplitude may be taken as the value of $(u'_{rms}/U)_{FW}$

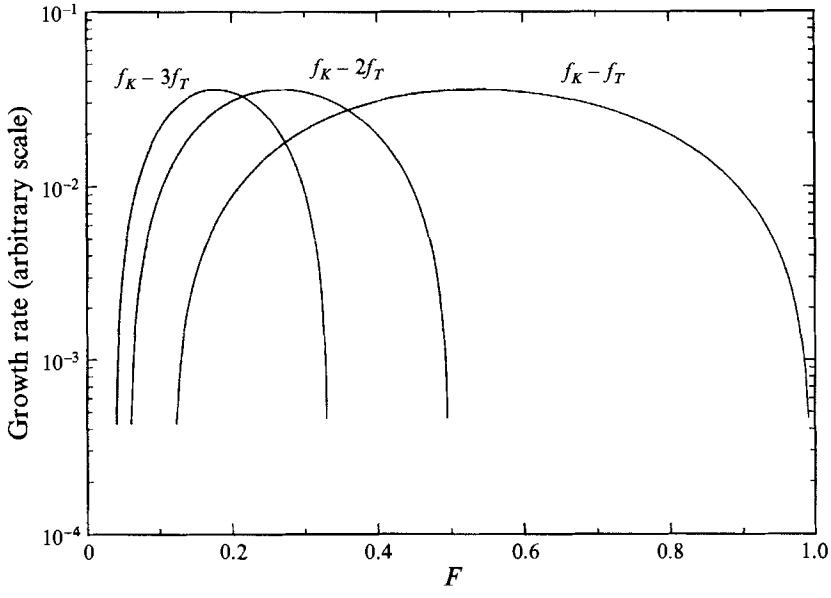

FIGURE 25. Growth rate curves for various oblique modes, versus forcing frequency F. These data for the spatial growth rate show the regions of normalized frequency over which one might expect each oblique resonance mode to be prominent. The vertical scale is arbitrary, and is simply to demonstrate the shape of the predicted growth rates.

evaluated at the point where the decaying energy of the oblique shedding waves equals the growing energy of the secondary mode, which is here defined as the start of the 'far wake'. For the case when $F = 0.55$, this wake amplitude response has been plotted as a function of the forcing amplitude A, in figure 23, and this shows the expected rise in response amplitude as A increases. However, it is interesting to note the reasonable agreement of the data with the relationship $(u'_{rms}/U)_{FW} = \text{const.} \times A^{\frac{1}{2}}$. In the limited cases computed, it was also found that the saturation amplitudes of the first oblique mode varied as $A^{\frac{1}{2}}$.

7. Discussion

Despite the fact that the oblique wave resonance is a nonlinear phenomenon, we can make useful comparisons between the observed phenomena and the predictions from stability analysis, following the spatial inviscid linear stability analysis of Cimbala (1984) and Cimbala *et al.* (1988), as used in WP. In this forcing study, we shall investigate only the maximum-response case $F = 0.55$, for which the most amplified frequency measured in the wake (as it travels downstream) is compared to the predictions from stability analysis in figure 24. It can be seen that for this amplitude ($A = 0.002$), the oblique shedding frequency gives way to the oblique resonance wave frequency ($f_K - f_T$) at around $x/D = 70$. This corresponds, approximately, to a drop in prominent frequency to a value predicted to have the maximum growth rate from the local theory, as noted in WP and Cimbala *et al.* (1988). However, in this case it appears that there are no other prominent frequencies which will take over as the most amplified frequency. The first oblique waves will grow and decay, and will dominate at all distances downstream, unless other forcing frequencies come into play.

A plot of growth rates for the different resonance modes can be derived from the analysis of Cimbala *et al.* in figure 25, where spatial growth rate on a logarithmic scale

is plotted versus predicted normalized forcing frequency F. The data have been calculated using values of wake defect velocity and wake width corresponding to a location at $x/D = 150$, and for $Re = 150$. Broad regions of wake response are found for each of the resonance modes. The ranges of F for which each of the modes is prominent appear to be approximately similar to the experimental measurements in figure 8.

It was shown in WP that Matsui & Okude's (1981) experiments involved a combination frequency resonance $(f_K - f_T)$ which was caused, for their particular wind tunnel, by a free-stream spectral peak at frequency $(f_T D^2/\nu) = 13.8$. This free-stream frequency 'controlled' the predominant far-wake frequency over a range of $Re = 100$–160. Combination frequency response of the wake to specific free-stream conditions has also been observed by Cimbala & Krein (1990), who influenced the free-stream spectrum by opening and closing vents downstream of the test section, for $Re = 140$. In their case, there was more than one prominent peak in the free-stream spectrum, which induced a rather complex multi-peaked wake response, although particular combination frequencies could clearly be seen. A further study by Desruelle (1983) showed that, by acoustic forcing, a combination frequency response $(f_K - f_T)$ occurred in the far wake $(x/D = 200)$, over a large range of $F = 0.32$–0.84. The above studies show that a resonance at combination frequencies involving free-stream noise is a common feature of wind tunnel facilities. In fact, in all of the above studies the combination-frequency response can far exceed the free-stream noise frequency response itself, in agreement with the present work.

8. Conclusions

This work follows from an earlier study in which we observed the exquisite sensitivity of the 'natural' far wake to the disturbances present in the free stream (Williamson & Prasad 1993*a*). Indeed, it was found that it is, surprisingly, the noise in the free stream which forms the 'connection' between near and far wakes, enabling the far wake to exhibit a 'signature' of the near-wake vortex structure, and causing the regular three-dimensional wave patterns that may be observed. Our central question, in this paper, is not so much whether the near and far wakes are 'connected' by both their frequencies and scale; it is to what extent the character of the free-stream noise may enhance or camouflage the far-wake 'signature' of the near wake.

In the present paper, we have induced nonlinear oblique wave resonance in the far wake by the use of (paradoxically) two-dimensional wave acoustic forcing of the free stream. A set of oblique resonance modes has been found, which corresponds to frequencies $(f_K - nf_T)$, where n is an integer. These oblique resonances are distinctly different from the subharmonic resonance models that have hitherto been used to represent the far wake.

Flow visualization shows that the far wake responds to the interaction of the two-dimensional forcing with the oblique shedding waves by exhibiting oblique resonance waves $(f_K - nf_T)$ over a surprisingly wide range of normalized forcing frequencies, $F = (f_T/f_K)$. Even under conditions where the oblique and two-dimensional secondary waves have the same frequency, and when linear analysis might suggest two-dimensional waves to be prominent, the visualization clearly demonstrates the preferential amplification of the oblique resonance waves.

The response of the wake, to a large range of forcing frequencies, shows a broad region of peak response, centred around $F = 0.4$–0.45, for the first oblique resonance mode $(f_K - f_T)$. The measurements also show that a second resonance $(f_K - 2f_T)$ and a third resonance $(f_K - 3f_T)$ exhibit peak responses at lower values of F. However, the

actual frequency most amplified in the far wake, for all these higher-order oblique modes, is broadly between 0.4–0.5 of the oblique shedding frequency, which is close to the frequency for maximum growth rate (0.457) that may be predicted from linear stability analysis. The variations of theoretical growth rates for the different oblique resonances ($f_K - nf_T$), over a range of F, have a distinctly similar appearance to the measured wake responses for these oblique modes.

Equations for the geometry of the resonance waves are simply derived, one of which shows that the spanwise wavelengths of all the oblique wave systems are the same, and are exactly equal to the spanwise wavelength of the oblique shedding waves. Use of these equations yields conditions under which peak response of the far wake may be predicted, if we make the approximation that peak response occurs for $F = 0.5$. The frequencies for peak response correspond to

$$F_{max} = \frac{1}{2n} = \tfrac{1}{2}, \tfrac{1}{4}, \tfrac{1}{6} \cdots,$$

which is approximately what is found from the response curves. An estimate for the oblique wave angles for maximum wake response is given by

$$\theta_{max} = 2\theta_K,$$

where θ_K is the oblique shedding angle. For typical oblique shedding angles of around 15° in different facilities, one may thus expect to observe prominent resonance wave angles of around 30°. In the present work, for large values of F, resonance for oblique waves of remarkably large angle (relative to the two-dimensional waves) up to $\theta_1 = 74°$ has been observed.

An increase of forcing amplitude has the effect of bringing the nonlinear interactions, which lead to oblique wave resonance, further upstream. Surprisingly, as one increases the amplitude of the two-dimensional wave forcing, the net effect of the nonlinear interactions is to further amplify the oblique resonance waves, in preference to the two-dimensional waves. In the case of low F, differences in forcing amplitude can lead to a change in the sequence of oblique or two-dimensional wave modes that become prominent as the wake travels downstream. With a variation in forcing amplitude (A), the amplitude of oblique wave response is found to be closely proportional to $A^{\frac{1}{2}}$.

This study of acoustic forcing of the far wake confirms that the signature of the near wake left in the far wake is dependent on the noise in the free stream. This particular work has shown the response of the far wake to single-frequency acoustic forcing, and we are presently investigating other forms of disturbance to the free stream. A fundamental question that guides our study is to what extent the character of the free-stream spectrum enhances or camouflages the signature of the near wake that is carried downstream.

At present, an analytical and computational effort is underway to describe the above wave interactions, and to resolve some of the outstanding questions. As one part of this effort, we are collaborating with Dr Alain Pumir at the Institut Nonlineaire, Université de Nice, concerning analysis of stability and a description of the wave interactions in terms of coupled amplitude equations.

The authors would like to thank Gregory D. Miller at Cornell for his invaluable help setting up the acoustic forcing technique, and for the Beethoven video presentation. Thanks are due for the hearty encouragement received from Professors Sidney Leibovich and Philip Holmes at Cornell. The authors thank also Chantal Champagne,

PhD, for indispensable assistance during paper preparation. This work was supported at Cornell by an ONR Contract No. N00014-90-J-1686, as part of the ONR 'Bluff body Wake Vortex Dynamics and Instabilities' Accelerated Research Initiative.

REFERENCES

CIMBALA, J. M. 1984 Large structure in the far wakes of two-dimensional bluff bodies. PhD thesis, Graduate Aeronautical Laboratories, California Institute of Technology.

CIMBALA, J. M. & KREIN, A. 1990 Effect of freestream conditions on the far wake of a cylinder. *AIAA J.* **28**, 1369.

CIMBALA, J. M., NAGIB, H. M. & ROSHKO, A. 1988 Large structure in the far wakes of two-dimensional bluff bodies. *J. Fluid Mech.* **190**, 265.

CORKE, T., KRULL, J. D. & GHASSEMI, M. 1992 Three-dimensional mode resonance in far wakes. *J. Fluid Mech.* **239**, 99.

DESRUELLE, D. 1983 Beyond the Karman vortex street. MS thesis, Illinois Institute of Technology, Chicago.

EISENLOHR, H. & ECKELMANN, H. 1989 Vortex splitting and its consequences in the vortex street wake of cylinders at low Reynolds number. *Phys. Fluids* A **1**, 189.

FLEMMING, M. F. 1987 Secondary instability in the far wake. MS thesis, Illinois Institute of Technology, Chicago.

HAMMACHE, M. & GHARIB, M. 1989 A novel method to promote parallel shedding in the wake of circular cylinders. *Phys. Fluids* A **1**, 1611.

HAMMACHE, M. & GHARIB, M. 1991 An experimental study of the parallel and oblique vortex shedding from circular cylinders. *J. Fluid Mech.* **232**, 567.

HAMMACHE, M. & GHARIB, M. 1992 On the evolution of three-dimensionalities in laminar bluff body wakes. In *Proc. IUTAM Conf. on Bluff Body Wake Instabilities* (ed. H. Eckelmann & J. M. R. Graham). Springer (to appear).

KOENIG, M., EISENLOHR, H., ECKELMANN, H. 1990 The fine structure in the *S–Re* relationship of the laminar wake of a circular cylinder. *Phys. Fluids* A **2**, 1607.

LASHERAS, J. C. & MEIBURG, E. 1990 Three-dimensional vorticity modes in the wake of a flat plate. *Phys. Fluids* A **2**, 371.

MATSUI, T. & OKUDE, M. 1981 Vortex pairing in a Karman vortex street. In *Proc. Seventh Biennial Symp. on Turbulence, Rolla, Missouri.*

MATSUI, T. & OKUDE, M. 1983 Formation of the secondarty vortex street in the wake of a circular cylinder. In *Structure of Complex Turbulent Shear Flow, IUTAM Symp., Marseille, 1982.* Springer.

MEIBURG, E. 1987 On the role of subharmonic perturbations in the far wake. *J. Fluid Mech.* **177**, 83.

MEIBURG, E. 1992 The three-dimensional evolution of oblique waves in plane wakes. In *Proc. IUTAM Conf. on Bluff Body Wake Instabilities* (ed. H. Eckelmann & J. M. R. Graham). Springer (to appear).

SQUIRE, H. B. 1933 On the stability for three-dimensional disturbances of viscous fluid flow between parallel walls. *Proc. R. Soc. Lond* A **142**, 621.

TANEDA, S. 1959 Downstream development of wakes behind cylinders. *J. Phys. Soc. Japan* **14**, 843.

WILLIAMSON, C. H. K. 1988 Defining a universal and continuous Strouhal–Reynolds number relationship for the laminar vortex shedding of a circular cylinder. *Phys. Fluids* **31**, 2742.

WILLIAMSON, C. H. K. 1989 Oblique and parallel modes of vortex shedding in the wake of a circular cylinder at low Reynolds numbers. *J. Fluid Mech.* **206**, 579.

WILLIAMSON, C. H. K. 1992 Wave interactions in the far wake. In *Proc. IUTAM Conf. on Bluff Body Wake Instabilities* (ed. H. Eckelmann & J. M. R. Graham). Springer (to appear).

WILLIAMSON, C. H. K. & PRASAD, A. 1993*a* A new mechanism for oblique wave resonance in the 'natural' far wake. *J. Fluid Mech.* **256**, 269 (referred to herein as WP).

WILLIAMSON, C. H. K. & PRASAD, A. 1993*b* Oblique wave interactions in the far wake. *Phys Fluids* A **5**, 1854.